View metadata, citation and similar papers at core.ac.uk

brought to you by CORE

provided by NASA Technical Reports Server

General Disclaimer

One or more of the Following Statements may affect this Document

- This document has been reproduced from the best copy furnished by the organizational source. It is being released in the interest of making available as much information as possible.

- This document may contain data, which exceeds the sheet parameters. It was furnished in this condition by the organizational source and is the best copy available.

- This document may contain tone-on-tone or color graphs, charts and/or pictures, which have been reproduced in black and white.

- This document is paginated as submitted by the original source.

- Portions of this document are not fully legible due to the historical nature of some of the material. However, it is the best reproduction available from the original submission.

Produced by the NASA Center for Aerospace Information (CASI)

NASA CR 73,307

Final Report

STUDY OF PIONEER SPACECRAFT OSCILLATOR STABILITY

By Howard C. Salwen

November 1968

Prepared under Contract No. NAS2-5021

For

AMES RESEARCH CENTER
National Aeronautics and Space Administration
Moffett Field, California

Distribution of this report is provided in the interest of information exchange. Responsibility for the contents resides in the author or organization that prepared it.

FACILITY FORM 602

N 69-23416 (ACCESSION NUMBER) (THRU)
41 (PAGES) 1 (CODE)
CR-73307 (NASA CR OR TMX OR AD NUMBER) 07 (CATEGORY)

ADVANCED COMMUNICATIONS INFORMATION MANAGEMENT

RESEARCH • DEVELOPMENT • ENGINEERING

ADCOM

A TELEDYNE COMPANY

NASA CR 73,307

Final Report

STUDY OF PIONEER SPACECRAFT OSCILLATOR STABILITY

by Howard Salwen

November 1968

Contract NAS2-5021

Prepared for

National Aeronautics and Space Administration
Ames Research Center
Moffett Field, California 94035

Distribution of this report is provided in the interest of information exchange. Responsibility for the contents resides in the author or organization that prepared it.

By

ADCOM
A Teledyne Company
808 Memorial Drive
Cambridge, Massachusetts 02139

TABLE OF CONTENTS

TABLE OF CONTENTS (Continued)

LIST OF ILLUSTRATIONS

1. INTRODUCTION

This document constitutes the final report prepared by ADCOM, a Teledyne Company, for NASA, Ames Research Center, under Contract No. NAS2-5021 entitled Study of Pioneer Spacecraft Oscillator Stability.

1.1 Background

The object of the study program is the determination of spacecraft oscillator stability characterization for optimization of overall Pioneer telemetry link performance. Specifically, the analytic relationship between Pioneer telemetry link performance, as indicated by bit error rate, and the short-term stability characteristics of the Pioneer spacecraft radiated carrier is investigated.

Spacecraft oscillator instabilities effectively broaden the spectral components of the spacecraft transmitted signal. This broadening tends to degrade the data demodulation process under certain conditions. These occur when the Pioneer vehicle is at extremely long range. The conditions under which data detection performance is degraded by carrier instability are illustrated by straightforward consideration of the data demodulation technique employed by the Pioneer link. At the ground station, the carrier component of the signal received from the spacecraft is tracked by a phase-locked loop which constitutes a coherent demodulator. In particular, the reference signal of the PLL is used to coherently demodulate the PM data. Clearly, it is necessary for the PLL to track the received carrier closely in order to maintain the desired coherence. This requires some dynamic capability of the PLL which is readily established by providing sufficient PLL bandwidth. Unfortunately, increasing the PLL bandwidth results in increased errors due to noise. These conflicting requirements on PLL bandwidth are embodied in a well-known tradeoff procedure in which a PLL bandwidth is determined which minimizes a suitably chosen combination of noise and dynamic errors.

Typically, such tradeoff analyses are concerned with dynamic tracking requirements as imposed by vehicle (e.g. spacecraft) motion. However, in those cases where vehicle dynamics are negligibly small or where they are known, a priori, (and therefore may be removed by other means) carrier oscillator instabilities become the predominant source of dynamic tracking requirements. The amount of noise reduction obtained in the receiver's carrier tracking loop is thus limited by the conflicting dynamic tracking requirements imposed by carrier instabilities.

Experience with the Pioneer link indicates that very narrow PLL tracking bandwidths are required when the vehicle is at extremely long range, i.e., when the SNR is poor. For this reason, the nature and effect of carrier instabilities in the Pioneer telemetry link are investigated. In this way, optimum PLL tracking bandwidth in the presence of noise and carrier instability can be established thereby minimizing the effect of carrier PLL errors on the data detection process.

1.2 Contents of the Report

Section 2 disucsses the effect of oscillator instability on coherent demodulator performance. There, oscillator instability is characterized, the relationship between oscillator instability and coherent demodulator performance is established, and estimates of carrier lock error due to oscillator instabilities in the Pioneer system are presented. In addition, an experimental method for measuring oscillator short-term stability is discussed.

The results of Sec. 2 may be used to determine rms carrier lock error and the consequent reduction in the average power of the demodulated signal, assuming that the PLL of the coherent demodulator remains in the linear region. Sec. 3 goes on to consider non-linear effects. Specifically, the effect of carrier unlock on bit error rate is analyzed.

Section 4 summarizes the results of the study program and presents conclusions and recommendations.

2. EFFECT OF OSCILLATOR INSTABILITY ON COHERENT DEMODULATION PERFORMANCE

2.1 Introduction

This section discusses the effect of oscillator instability on coherent demodulator performance. Specifically, the general character of oscillator instabilities is discussed, and the relationship between oscillator instability and carrier PLL lock error is discussed. Then, the effects of the oscillator instabilities associated with the Pioneer telemetry link are presented in the form of coherent demodulator carrier lock error as a function of carrier loop noise bandwidth. The effect of a carrier loop error, ϕ_ϵ, is to reduce the average detected energy per bit by a factor of $\overline{(\cos \phi_\epsilon)}^2$.

2.2 The Effect of Oscillator Instability on Coherent Demodulator Performance

For the purposes of analysis, the instability of an oscillator is most conveniently expressed in terms of the power density spectrum of its phase or frequency fluctuations.[1] In particular, the output of an oscillator may be described by

$$e_{osc}(t) = A \cos(2\pi \bar{f} t + \phi_i(t))$$

where A is an arbitrary constant, $\bar{f}$ is the long term average frequency output of the oscillator, and $\phi_i(t)$ represents the zero mean random phase fluctuations of the oscillator. The power density spectrum of these phase fluctuations is typically denoted by $S_\phi(\omega)$ and, of course, the power density spectrum of the frequency fluctuations $S_\phi^{\cdot}(\omega)$ by

$$S_\phi^{\cdot}(\omega) = \omega^2 S_\phi(\omega)$$

In general, the power spectral density of an oscillator's phase fluctuations is composed of a number of terms, each of which is associated with a noise producing physical mechanism.

2.2.1 Physical Mechanisms and the Resulting Spectral Shapes[2-7]

There are four principal types of angular modulation effects produced by noise in oscillators. Any or all of them may be present in a particular oscillator. They may be grouped in one set of pairs by the type of noise and in another set of pairs by the region of the oscillator spectrum which is affected. The two types of noise are white noise, i.e., Johnson, shot or thermal, and perturbation noise which is often referred to as flicker noise. The two regions of the oscillator's spectrum are within and without the resonator's effective half bandwidth or $f < f_o/2Q$ and $f > f_o/2Q$.

The effect produced by white noise for $f < f_o/2Q$ is a flat FM noise spectrum, the physical mechanism for which can be thought of as the voltage to frequency transference of the oscillator through its feedback network. The effect produced by white noise for $f_m > f_o/2Q$ is a flat PM noise spectrum. This assumes a single pole resonator which is almost invariably the case for several reasons among which is the maximization of the effective Q. This single pole applies an f^{-2} weighting to the FM noise spectral components outside the oscillator's half bandwidth thus producing a flat PM spectrum. Alternatively, one can assume that since the phase shift vs. frequency characteristic of the resonator is nearly zero outside its bandwidth, then the voltage to frequency transference of the oscillator will be negligible in this region. Therefore flat white noise will appear directly as equally weighted flat AM and PM spectra. The magnitude of the flat PM mean square spectral density out of the oscillator itself is given by $2FKT/P$. F is the actual operating noise figure of the active element of the oscillator and includes all noise components folded into the passband from harmonics of the fundamental frequency. KT is -174 dBm/Hz.

P is the available power at the input of the active element of the oscillator. This flat PM spectrum extends out in frequency until it is attenuated by subsequent filtering.

The fundamental causes of flicker noise are not well understood. However, they appear to arise from random changes in physical parameters (such as charge density in a transistor) which manifest themselves as a rise in the effective noise figure of the device at low spectral frequencies. This rise in noise figure consistently obeys an f^{-1} law but it can vary widely in magnitude from one device to another. The effect produced by flicker noise for $f < f_o/2Q$ is an FM spectrum with an f^{-1} characteristic. This flicker FM spectrum has been shown to exist in crystal oscillators at spectral frequencies down to 3×10^{-7} Hz.[8] In high Q or low frequency oscillators where $f_o/2Q$ is small, the flicker noise region of the oscillator's active elements can extend into the spectral frequency region beyond $f_o/2Q$ thereby giving rise to a flicker PM spectrum. Under these conditions, since flicker noise extends indefinitely to lower spectral frequencies, the oscillator will not exhibit a region of flat FM spectrum.

In addition to the angular modulation effects produced by noise in an oscillator, there is an amplitude modulation noise spectrum. This appears as a flat AM spectrum for high spectral frequencies and is equal to the PM spectral level.[3] For low spectral frequencies, the angular modulation spectral density far exceeds the AM spectral density.

It is interesting to note that all physically realizable oscillators with the single exception of the cesium beam resonator have flicker FM noise spectra. The existence of flicker FM noise in the hydrogen maser is presently in question.[9]

There are two principal types of angular modulation effects produced by noise in signal processing circuits other than the oscillator circuit. These are

flat PM noise and flicker PM noise. There is also flat AM noise. These signal processing circuits can be divided into four classes.

1. Amplifiers, linear and nonlinear
2. Frequency multipliers
3. Mixers (modulators or multipliers)
   - A Frequency translators
   - B Zero frequency IF and phase detectors
4. Frequency dividers

The signal degradation which occurs in both linear and nonlinear amplifiers appears to be exclusively flat white noise. In linear amplifiers, this noise is inversely proportional to the signal-to-noise ratio, and is equally divided between AM and PM. If N_o/S is the noise density-to-signal ratio, then $2N_o/S$ is the PM spectral density. Where the amplifier noise figure and input signal power level are known, the PM density is given by 2 FKT/P. The AM modulation density is $200\ N_o/S = 200$ FKT/P percent. In nonlinear amplifiers, the effects of saturation provide appreciable suppression of the AM components. According to FM theory[10] the capture effect reduces the angular modulation of the weaker signal by about 6 dB. Therefore, the PM spectral density added to a signal by a nonlinear amplifier should be about 6 dB lower than the equivalent linear amplifier, providing the operating noise figure is the same.

The signal degradation produced by frequency multipliers appears to be the same as in nonlinear amplifiers. However, the PM spectral density out of the multiplier is higher by N^2 (or $20 \log_{10} N$), where N is the multiplication ratio. The AM spectral density is not increased by N. Therefore, the output of a multiplier for any appreciable N is exclusively PM. It should be noted that as the frequency multiplication ratio N is increased, the performance of a frequency multiplier rapidly approaches the ideal for the cases of diode, varactor,

and Class C type multipliers.[11] This occurs because the multiplier input phase noise, $S_\phi(\omega)$, is scaled up while the multipliers internally generated noise is not scaled. Thus, for large N, the scaled input noise predominates all other sources of noise at the output of the multiplier.

A mixer, which for this discussion is defined as performing the function $e_o(t) = e_1(t) \cdot e_2(t)$, has two regions of interest. The first is where $e_o(t)$ does not exist at or near DC, that is when the mixer is used as a frequency translator. For this condition, the performance is similar to that of an amplifier. Where one of the signals into the mixer is large compared with the other, the standard treatment for noise figure applies and the spectral density of PM noise is 2 FKT/P where F is the overall cascade noise figure. There is an equal amount of AM noise. Where the amplitude of both input signals is of similar magnitude then the performance is akin to that of a nonlinear amplifier. In both cases, the noise spectra (PM and AM) will be flat. The second region of interest is where the output spectrum is centered on DC, that is, where the mixer is operated in the homodyne or zero frequency IF condition, or as a phase detector. For this condition the inherent flicker noise of the diodes or other active elements contributes to the spectral distribution in many instances. This effect is well known, for example, in doppler radars where the effective noise figure in the range of a few Hz to several kHz is several orders of magnitude above that which is obtained using the same mixer as a frequency converter to an IF in the MHz region. The same problem exists in phase detectors when very high signal-to-noise ratios are desired. Typical values for excess PM and AM noise density at 1 Hz are 20 to 70 dB above KT/P. This is indeed flicker noise and obeys an f^{-1} law.

The signal degradation produced by frequency dividers comes from two sources, flicker PM and broadband white noise (AM & PM). The spectral density level of angular modulation out of an ideal frequency divider should be

that of the input divided by N^2 where N is the division ratio. However, the two sources of degradation in the divider tend to mask this improvement for high purity signals. The broadband white noise level is usually determined by the last divider or the first amplifier following it. There appears to be a considerable amount of flicker PM noise generated by both regenerative analog dividers and digital dividers. In digital dividers it is clear that the time jitter of the state transition in response to a zero crossing of the input signal is due to the same internal device fluctuations that produce flicker noise in oscillators. The resulting flicker spectrum of PM confirms this. The same effect appears to occur in regenerative analog dividers. In general, as the divider ratio N is increased, the noise inherent to the divider elements will begin to predominate over the scaled down input phase fluctuations.

2.2.2 Equations of Composite Spectra

For many applications, especially those where the signal is either multiplied in frequency or used for timing or ranging purposes, the effects of angular modulation fluctuations far outweigh those of amplitude modulation. For the case under consideration here, only the phase (or frequency) fluctuations are of interest.

The known physical processes discussed above produce only four distinct types of mean square spectral density, namely, flicker FM, flat FM, flicker PM, and flat PM. Therefore, it is possible to write equations for the spectral density of the PM fluctuations as:

$$S_\phi(\omega) = \frac{A}{\omega^3} + \frac{B}{\omega^2} + \frac{C}{\omega} + D \quad (\text{rad})^2/\text{Hz} \qquad (1)$$

where A is a constant associated with the magnitude of the frequency flicker noise, B is a constant associated with the magnitude of the frequency white noise, C is a constant associated with the magnitude of the phase flicker noise

and D is a constant associated with the magnitude of the phase white noise. More is said about experimental and theoretical values for these constants below and an experimental measurement system is described in Appendix A.

2.2.3 The Relationship Between Oscillator Fluctuations and PLL Error

A phase model of a phase-locked loop is shown in Fig. 1. A second order compensation is assumed. The phase fluctuations under consideration may be associated with either the input signal or the VCO output or both. The power density of error signal, $\epsilon(t)$, due to phase fluctuation $\phi_i(t)$ at the input to the PLL is given by

$$S_\epsilon(\omega) = |1 - H(\omega)|^2 S_\phi(\omega) \tag{2}$$

where $H(\omega)$ is the loop transfer function defined as

$$H(\omega) = \frac{K(1 + \tau_1 s)}{s(1 + \tau_2 s) + K(1 + \tau_1 s)}, \quad s = j\omega \tag{3}$$

and

$$1 - H(\omega) = \frac{s(1 + \tau_2 s)}{s(1 + \tau_2 s) + K(1 + \tau_1 s)}, \quad s = j\omega \tag{4}$$

Finally, the mean square value of the error signal, σ_ϵ^2 in $(\text{rad})^2$ is given by[12,13]

$$\sigma_\epsilon^2 = \frac{1}{2\pi} \int_{-\infty}^{\infty} S_\phi(\omega) |1 - H(\omega)|^2 \, d\omega \tag{5}$$

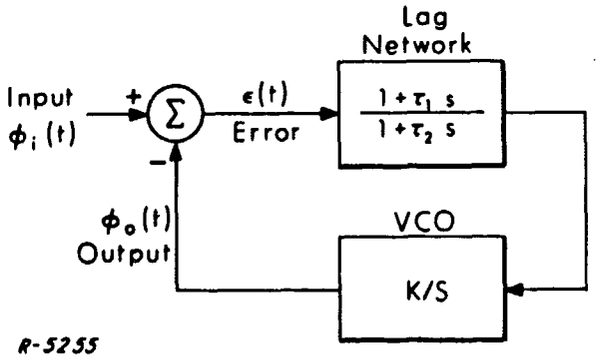

Fig. 1 Phase Model of a PLL

Two problems arise in evaluating the rms phase error, σ_ϵ. First, reasonable values or ranges of values for the coefficients of $S_\phi(\omega)$, namely A, B, C, and D, must be found. Then, having done this, the integral above must be evaluated. These operations are performed next.

2.3 Oscillator Characterization

The specific power spectral densities of phase fluctuations obtained from each of the oscillators used in establishing the PIONEER data link are not presently available. However, some theoretical and experimental data are available on oscillators similar to those employed in the PIONEER link. In the discussion below, bounds derived from these data are placed on the parameters of $S_\phi(\omega)$ which are of interest. It should be noted that the PIONEER link has two modes of operation, each of which has a distinct oscillator stability characterization. These characterizations are presented next and related to parameter values for $S_\phi(\omega)$.

2.3.1 Characterization of Modes of Operation

The open loop mode of operation is straightforward. A free-running crystal oscillator produces an output at approximately 20 MHz. This output is PSK modulated, multiplied up to S-band, and transmitted to the ground station. At the ground station, the received carrier is tracked in an IF PLL and the PSK data is demodulated by a coherent demodulator which employs the IF PLL reference signal. It is reasonable to assume that the predominant source of oscillator instability arises in the satellites oscillator and output circuitry rather than in ground station equipment because a substantially higher level of sophistication may be employed in the ground station equipment. On the other hand, size, weight, and power consumption restrictions on board the satellite limit the stability performance obtainable on the satellite downlink. Thus it is concluded that the predominant oscillator instabilities component at the coherent

demodulator for the open loop mode of operation is $N^2 S_{\phi o}(\omega)$ where $S_{\phi o}(\omega)$ is the power spectral density of phase fluctuations of the free running crystal oscillator on board the satellite and N is the multiplication ratio of the output chain in the satellite i.e., $N = 2 \times 3 \times 20 = 120$.

The closed loop transponder mode of operation is more difficult to analyze. In this case, the phase instabilities at the ground station coherent demodulator arise in part from noise at the input to the transponder, from instabilities in the transmitted uplink signal, and from instabilities of the VCO on board the satellite.* Specifically, for frequencies which are within the passband of the transponder closed-loop response, the instabilities at the output result from uplink signal instabilities and transponder input noise fluctuations which are tracked by the transponder VCO. Outside the transponder passband the instabilities at the output result from transponder VCO instabilities.

Assuming a signal-to-noise spectral density S/N_o at the input to the transponder, the phase noise density at the output is

$$\phi_n = \frac{N_o}{2S} |H(\omega)|^2 = \frac{N_o}{2S} K_o^2 |F(\omega)|^2 \tag{6}$$

where, from an examination of the pioneer circuitry, $K_o = 120/110.5$, and

$$F(s) = \frac{110.5K(1 + \tau_1 s)}{s(1 + \tau_2 s) + 110.5K(1 + \tau_1 s)} \tag{7}$$

$$K \approx 3 \times 10^6$$

$$\tau_1 \approx 7 \times 10^{-2}$$

$$\tau_2 \approx 1.2 \times 10^{-3}$$

The output phase fluctuations caused by instabilities of the uplink transmitted signal have density ϕ_t, given by,

$$\phi_t = S_{\phi t}(\omega) K_o^2 |F(\omega)|^2 \tag{8}$$

*The closed loop transponder also employs a reference oscillator. However, the effect of instability of this oscillator does not appear at the transponder output.

where $S_{\phi t}(\omega)$ is the transmitted carrier phase spectral density. Finally, the density of phase fluctuations at the transponder output caused by a VCO instability characterized by $S_{\phi v}(\omega)$, is given by

$$\phi_v = N^2 S_{\phi v}(\omega) |1 - F(\omega)|^2 \quad (9)$$

where N is the ratio of the output frequency to the VCO frequency.

In summary, a careful and exact evaluation of the carrier lock error due to oscillator instability in the PIONEER data link requires knowledge of the characteristics of three oscillators. (For the sake of argument, let us assume that the S/N_o at the input to the transponder is such that ϕ_n is negligible thereby emphasizing the effect of oscillator instabilities.) The power spectra of phase fluctuation for each of the oscillators is of the same form, namely, that given by Eq. (1). However, the values of each of the coefficients, A, B, C, and D will vary from oscillator to oscillator depending on technique and application. In order to compare the coefficients associated with different oscillators, it is necessary to normalize them with respect to oscillator output frequency. For this purpose, all values for coefficients in the discussion below are referenced to a 1 MHz oscillator output frequency.

2.3.2 Estimates of Oscillator Parameters

The coefficients of the frequency and phase flicker noise, A and C, are a function of the amount of parameter variation which physically occurs within the oscillator circuitry and the sensitivity of output frequency to parameter variation. Thus, it is reasonable to expect that oscillators in well controlled environments would have lower flicker noise than oscillators of the same type in poor environments. Furthermore, oscillators operating at relatively low frequency should have lower flicker noise than similar types operating at higher frequencies.

A theoretical investigation of the characteristics of a precision quartz 5 MHz reference standard[14] yielded the result that the frequency flicker coefficient referenced to 1 MHz is approximately $A = 4 \times 10^{-9}$. This result is based on published data for the particular oscillator. Laboratory experiments with a similar precision quartz crystal oscillator indicate a coefficient on the order of $A = 5 \times 10^{-9}$. Data is available for a quartz oscillator with fundamental at 100 MHz.[15] A for this oscillator is approximately 6.2×10^{-7}.

The oscillator used during open loop operation of the PIONEER link has a 20 MHz fundamental and it is assumed to be in a relatively uncontrolled environment. Therefore, the coefficient of the frequency flicker noise in this mode of operation is assumed to be on the order of 5×10^{-7} (ref. to 1 MHz). On the other hand, the flicker component in the closed loop mode is associated with the transmitter's instabilities. Assuming that the transmitted carrier is referenced to a laboratory standard, A is estimated to be on the order of 5×10^{-9} in this mode.

The next important component in $S_{\phi}(\omega)$ generally is caused by white frequency noise. The coefficient B referenced to the oscillator's fundamental frequency is given by

$$B = \left(\frac{\omega_o}{2Q}\right)^2 \frac{2FKT}{P} \tag{10}$$

Note that $2\,FKT/P = 2N_o/S = D$, the last coefficient in $S_{\phi}(\omega)$. It is therefore more convenient to present values for D before discussing estimates of B.

Theoretical analysis of a precision quartz crystal oscillator[14] has shown that the phase noise power density D was on the order of 10^{-13} (referenced to 1 MHz). This analysis was for the most part confirmed by experimental investigation of similar oscillators. The experimental data showed that the average phase noise density was 10^{-13}. All oscillators tested were within 10 dB of this figure. Thus, for the purposes of estimating values for B, D is

assumed to be on the order of 10^{-13}. Note that B is also a function of oscillator resonator Q. Estimates of Q are based on resonator type, e.g., LC, quartz crystal, cesium beam, etc., and on oscillator functional requirements. In particular, stable fixed sources may be designed with very high Q resonators while for the case of VCO's, the resonator Q is a function of VCO deviation requirements.

Based on the discussion above three distinct estimates of B for the three oscillators used in the PIONEER link are suggested. The transmitter reference oscillator should have the lowest value of B. Experimental evidence on reference standard oscillators indicates that B for such oscillators is on the order of 8×10^{-9} (refer to 1 MHz). This implies a loaded Q on the order of 55,000 at 5 MHz in the oscillator circuit with $D \approx 10^{-13}$. The reference oscillator on board the vehicle which is used to generate the open loop mode carrier will have a larger value of B since it operates at 20 MHz. If it is further assumed that this oscillator employs a resonator with lower Q, say, on the order of 25,000, then the value of B would be more than two orders of magnitude larger than that cited above for the reference standard. The VCO employed in the closed loop mode could have an even larger value of B if frequency deviation requirements indicated the necessity for lowering the resonator Q further. However, for the particular configuration under consideration, the deviation ratio required is equal to the ratio of uplink doppler offset to uplink carrier frequency, i.e., $fd/f_o = v/c$. Assuming that this ratio does not exceed 1×10^{-4}, the value of B for the VCO is assumed equal to that of the open loop carrier oscillator.

A value for C will not be estimated because, more often than not, this type of noise is obscured by the other noise components at the oscillator output. In fact, there is very little data in the literature concerning this type of noise and its origins are controversial. It is assumed in the calculations below, that

the frequency white noise (B type) predominates over the phase flicker noise (C type) at least over the frequency range of interest.

A summary of the range of values of the power spectral densities of phase fluctuations appropriate to the PIONEER links is shown in Fig. 2. The spectral densities are shown over the range of frequencies relevant to the evaluation of PLL lock in the coherent demodulator of the PIONEER receiver.

2.4 Evaluation of Carrier Lock Error

Substitution of the $S_\phi(\omega)$ of Fig. 2 into Eq. (5) is not straightforward. Examination of Eq. (4) shows that at very low frequencies, the integrand is proportional to $d\omega/\omega$. Thus, the integral will not converge. This problem is typically handled[16] by avoiding the region hear $\omega = 0$. The rationale for this approach is as follows: First, firm data on the character of oscillator instabilities is not available below $\omega = 10^{-8}$, i.e., for averaging time much longer than a year. Second and more important, the duration of any reasonable experiment is much shorter than a year and the duration of the experiment acts as a high-pass filter. In any case, the linear model for the PLL assumed in the derivation of Eq. (5) breaks down well before the mean square lock error becomes infinite. In the process of evaluating the integral of Eq. (5) it was found that if the region $|\omega| < 10^{-10}$ was excluded from the calculation, the divergent component of the integrand contributed negligibly to the total mean square error. Therefore, this component was ignored. Deletion of this troublesome term in Eq. (5) has been implicitly assumed by other investigators[12,13] in the field.

Further examination of Eqs. (4) and (5) shows that the integral will not converge due to high frequency effects. In particular, at high frequency $|1 - H(\omega)|^2$ approaches one and $S_\phi(\omega)$ is a constant. If the upper limit of the integral is $\omega = \infty$ then the integral will not converge. This problem may be handled in a manner similar to that employed above. That is, the practical aspects of the experiment must be considered and accounted for. To this end,

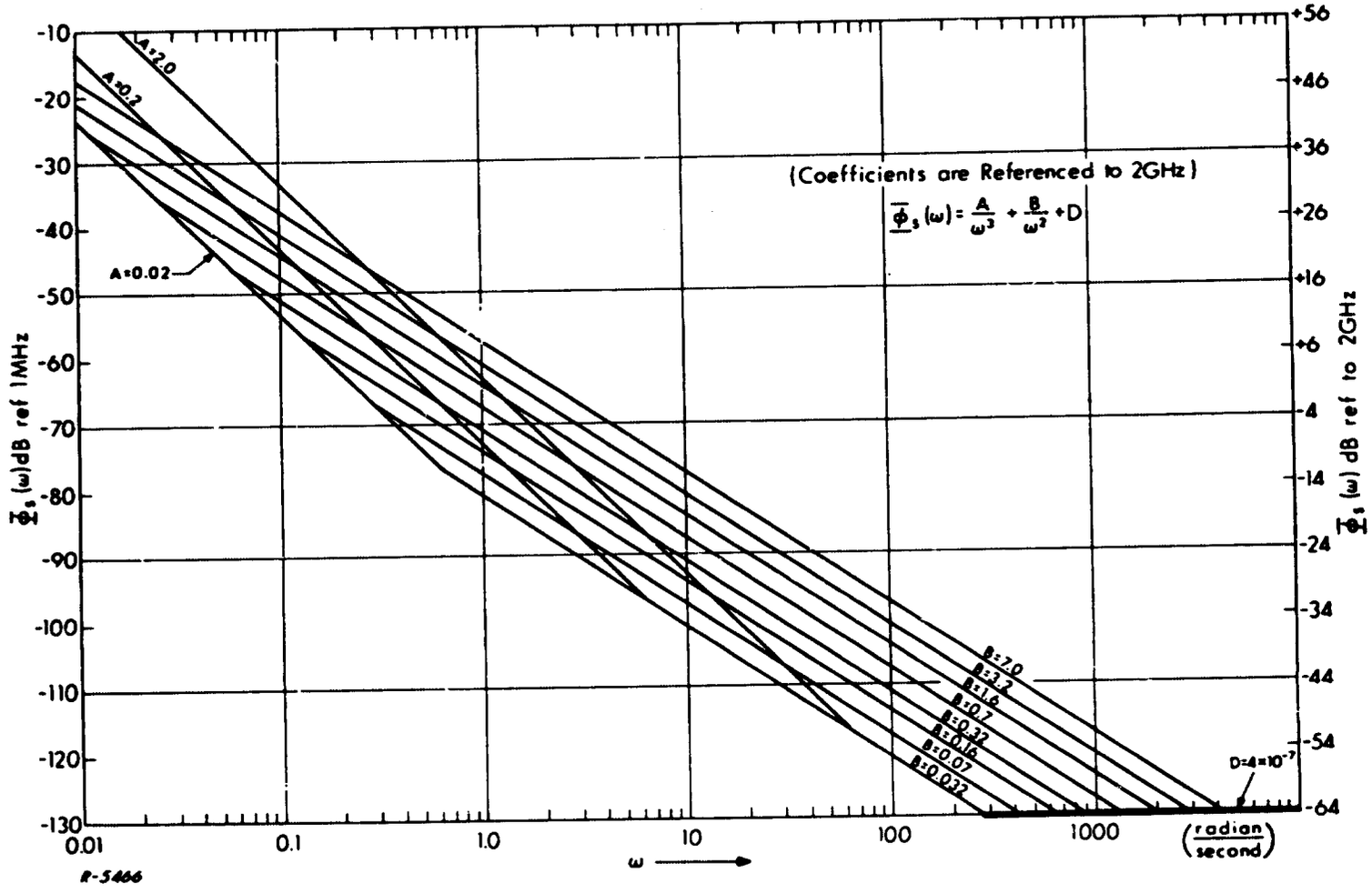

Fig. 2 Power Spectral Densities of Phase Fluctuation

note that the spectrum of phase fluctuations is affected by filters throughout the system not just the closed loop response characteristic of the PLL. The roll-offs introduced by IF filter characteristics and by lowpass filtering (other than the loop compensating network) at the phase detector of the PLL are accounted for in the calculation below by ignoring the phase noise component, D, in $S_\phi(\omega)$. This is essentially equivalent to lowpass filtering the phase fluctuations with a single pole filter with cutoff frequency defined by $\omega^2 = B/D$. Examination of Fig. 2 yields that the cutoff frequency is at least 40 cps for the cases under consideration here.

2.5 Results of the Analysis

The integral of Eq. (5) was evaluated with the aid of a digital computer for each of the 24 possible combinations of the parameters A and B shown in Fig. 2. The PLL was assumed to have a transfer function given by Eq. (4) with $K = 10^{6*}$ and damping set at 0.707. The noise bandwidth (double-sided) was varied over the range $0.1 < B_{nn} < 100$ cps. The results of the computation are shown in Figs. 3, 4 and 5.

*The results obtained are essentially independent of K for large K.

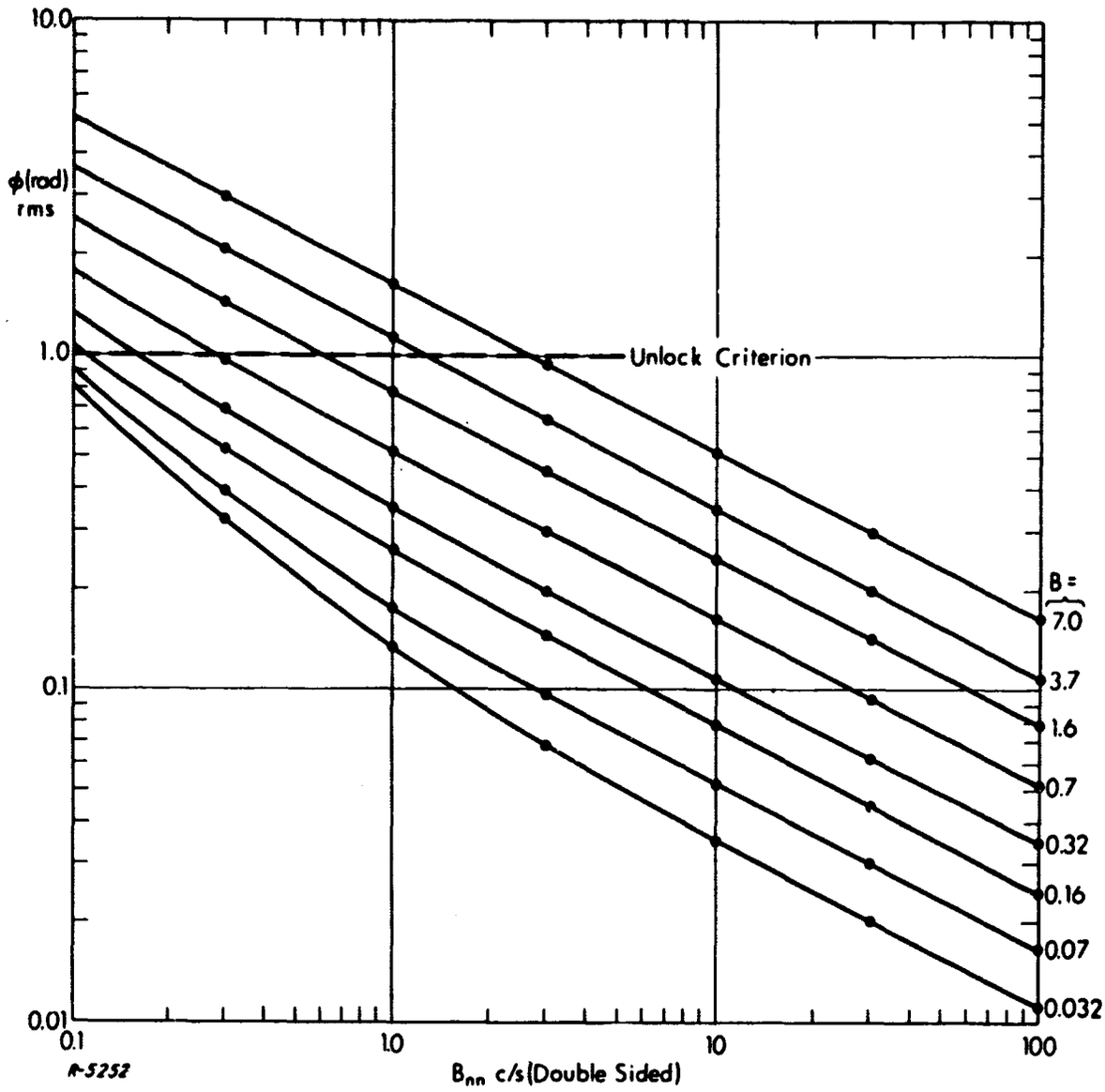

Fig. 3 Carrier Lock Error for A = 0.02

0.032 < B < 7

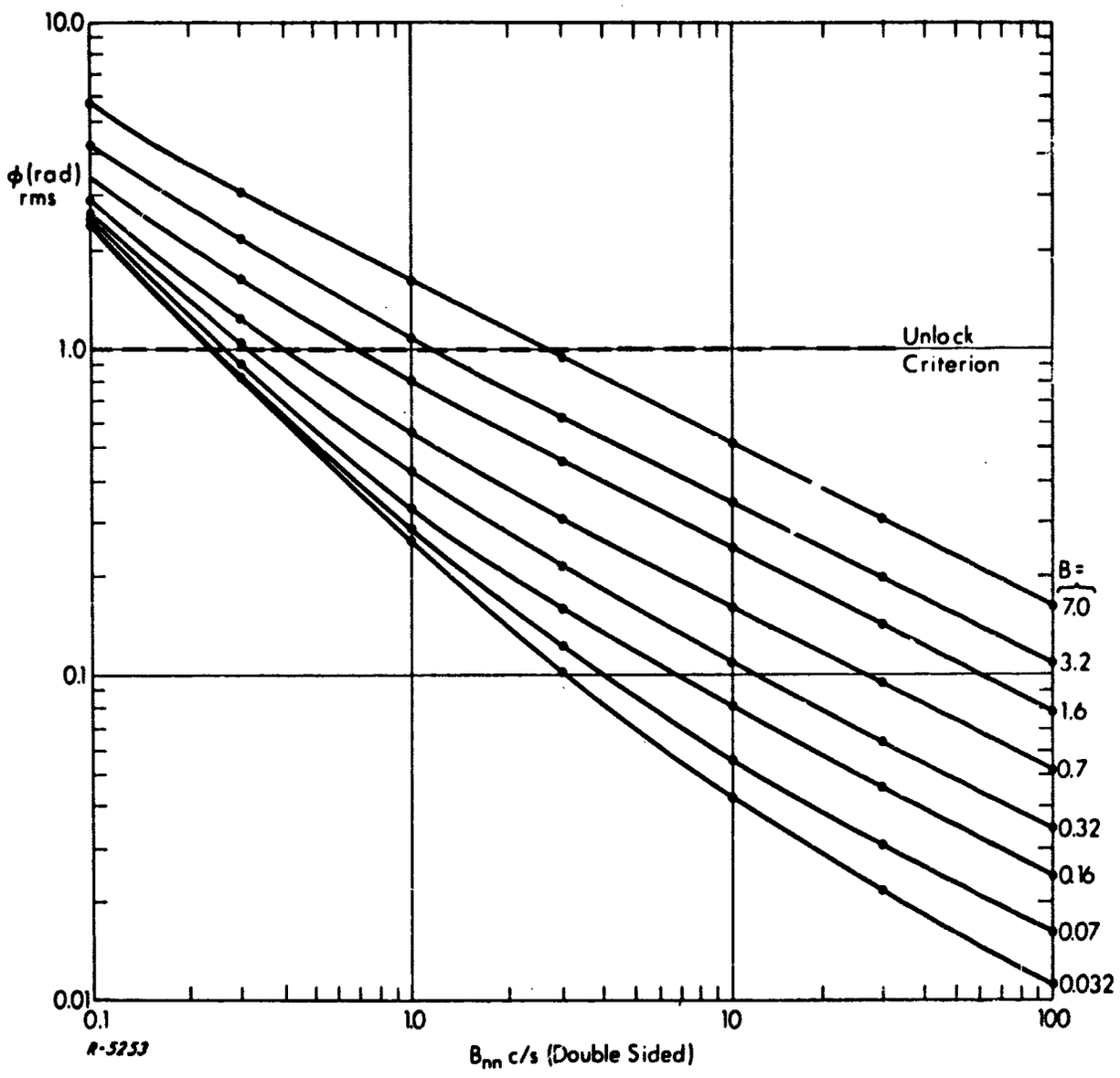

Fig. 4 Carrier Lock Error for A = 0.2

$0.032 < B \leq 7$

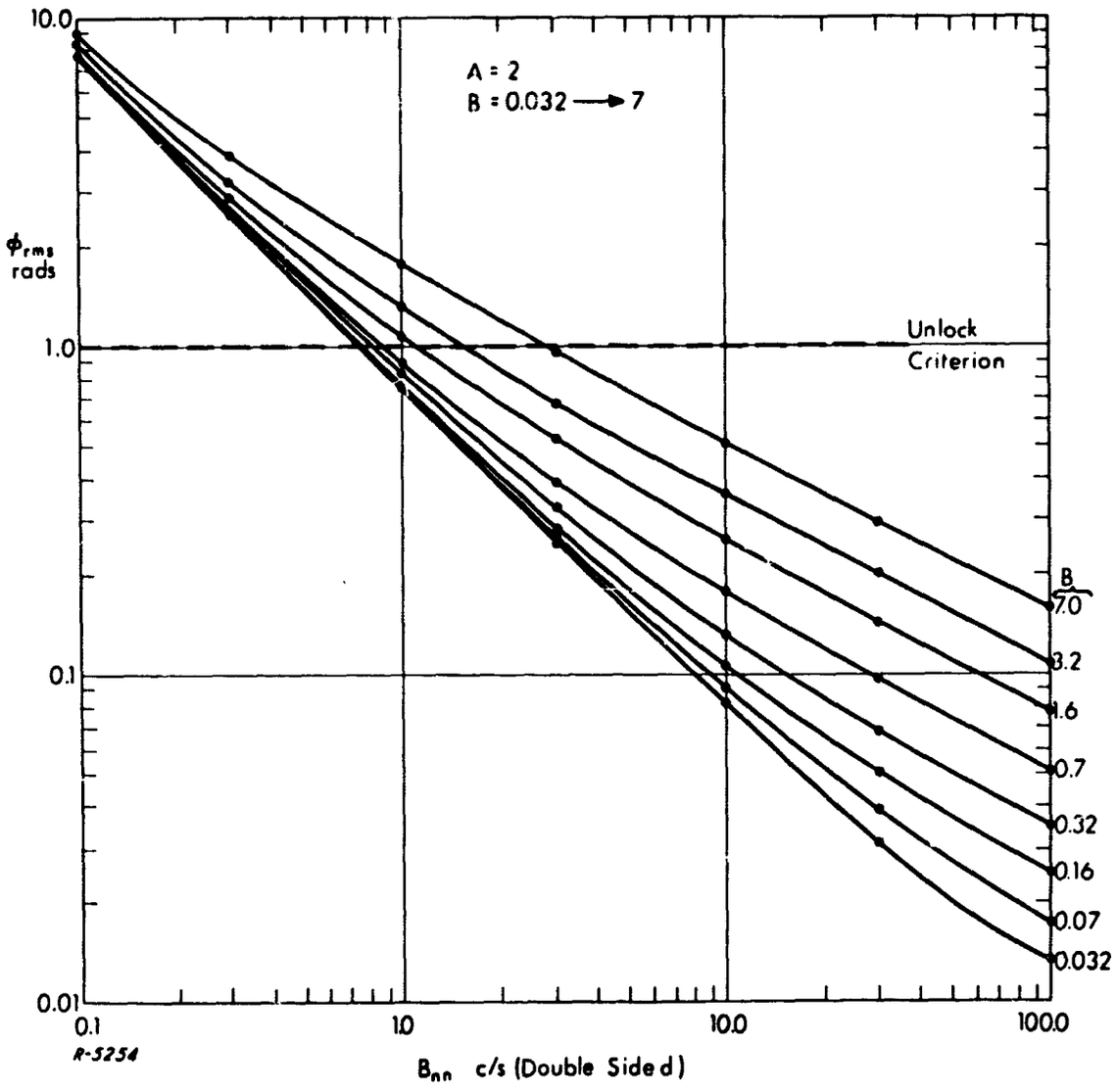

Fig. 5 Carrier Lock Error for A = 2

$0.032 < B \leq 7$

3. THE EFFECT OF CARRIER UNLOCK ON BIT ERROR PROBABILITY

3.1 Introduction

The results of Sec. 2 may be used to estimate the rms carrier PLL lock error due to oscillator instabilities as a function of carrier loop noise bandwidth, B_{nn}. This error, along with the errors due to noise and vehicle dynamics, appears at the output of the coherent demodulator. As long as the loop remains in the linear region, the effect of a carrier lock error is to reduce the average detected bit energy as described in Sec. 2.1. There is also the possibility that the loop will unlock if the carrier lock error gets large enough. This section considers the effect of carrier unlock due to noise on bit error. In this case, the total noise, N, is considered to consist of a random component due to receiver front-end noise and a random component due to transmitted carrier instabilities. It is shown that the effect of unlock will contribute substantially to the bit error rate when the SNR is low in the PIONEER telemetry link.

3.2 Unlock Effect

The calculation to determine the effect of unlock is based on an expression for the mean time to unlock which, for a 1/2 damped 2nd order PLL, is[17]

$$T_{av} = \frac{2}{B_{nn}} e^{\pi (S/N)_\ell} \tag{11}$$

where B_{nn} is the double sided noise bandwidth of the PLL and $(S/N)_\ell$ denotes the actual signal-to-noise ratio in the loop. Assume that after the loop unlocks it reacquires at the next available stable lock point, i.e., it slips at least one cycle relative to its input. Furthermore, assume that the mean time that the loop remains out of lock is inversely

proportional to B_{nn}, e.g., $T_{un} = K/B_{nn}$. Then, the relative frequency of being in a state of unlock is given by

$$P(\text{unlock}) \approx \frac{T_{un}}{T_{av}} = \frac{K}{2} e^{-\pi(S/N)_\ell}, \quad T_{av} > T_{un} \tag{12}$$

Next, determine the probability of error during unlock, P(e, unlock). It is noted that when the PLL is nearly locked P_e is small. When the carrier is exactly out of phase relative to the correct lock point the video output data at the coherent demodulator is inverted. Under these circumstances, $P_e = 1$ for the case of coherent PSK and P_e is small for the case of DPSK. Finally, when the PLL is roughly $\pm 90^o$ from the correct lock point, $P_e \approx 1/2$. On the basis of the heuristic analysis above, it is assumed that the probability of error given that the loop is unlocked and skipping cycles is, $P(e|\text{unlock}) = 1/2$.

The probability of error due to cycle skipping is, thus, found to be

$$P(e, \text{ unlock}) = P(e|\text{unlock})\, P(\text{unlock}) = \frac{K}{4} e^{-\pi(S/N)_\ell} \tag{13}$$

In order to plot a modified probability of error curve which includes the effect of sporadic carrier unlocks, the relationship between E_d/N_o in the data detector and $(S/N)_\ell$ in the carrier loop must be established. By definition

$$(S/N)_\ell = \frac{S}{N_o B_{nn}} \tag{14}$$

where S is the signal power in the loop, N_o is the double sided noise density. If a sinusoidal phase detector is assumed for both the carrier loop and the data detector and PSK deviation, δ, is assumed, then

$$(S/N)_\ell = \frac{S_o \cos^2 \delta}{N_o B_{nn}} \tag{15}$$

where S_o is the signal power at IF. Noting that the signal energy per bit

$$E = \frac{S_o \sin^2 \delta}{BR}, \tag{16}$$

where BR is the bit rate,

$$(S/N)_\ell = \frac{E(BR) \cos^2 \delta}{N_o B_{nn} \sin^2 \delta} \tag{17}$$

Finally, a slight degradation of video bit energy results from lack of perfect coherence of the demodulator reference signal. Thus, for an rms carrier lock error due to noise of ϕ_ϵ, the detected bit energy is

$$E_d = E\overline{(\cos \phi_\epsilon)^2} = E\, e^{-\phi_\epsilon^2} \tag{18}$$

Taking this last factor into account, the carrier loop $(S/N)_\ell$ is

$$(S/N)_\ell = \frac{E_d}{N_o} \frac{BR}{B_{nn}} \frac{\cos^2 \delta}{\sin^2 \delta\, e^{-\phi_\epsilon^2}} \tag{19}$$

Figure 6 shows a plot of the bit error rate vs E_d/N_o. Coherent PSK is assumed. The lowermost curve is the classical error probability, P_e, which does not include the effect of carrier unlocks. The other curves are plots of

$$P_{e_{Total}} = P_e + P(e,\ \text{unlock}) \tag{20}$$

for various assumed parameter values. Specifically, (BR) = 32 b/s and B_{nn} = 20 Hz are assumed in all cases. The ratio $(\cos^2 \delta / \sin^2 \delta) \exp(-\phi_\epsilon^2)$ is assumed to be either 2 dB or 3 dB and, finally, the mean duration of unlock is assumed to be either $4/B_{nn}$ or $8/B_{nn}$.

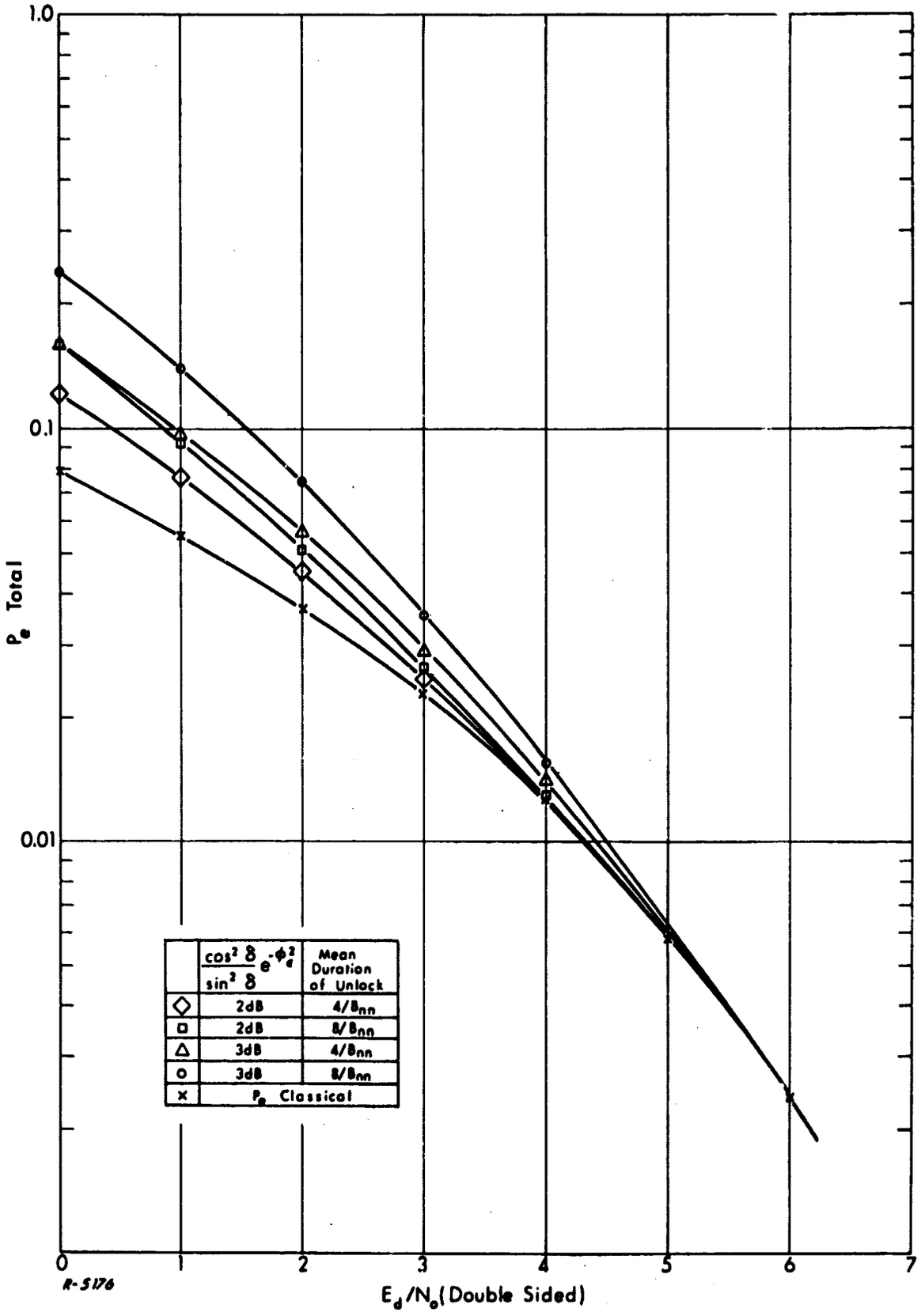

Fig. 6 Modified Bit Error Probability

4. RESULTS OF THE STUDY PROGRAM

4.1 Introduction

This section presents conclusions and recommendations based on the work performed under the referenced contract. The effort is divided into two broad categories which may be generally described as investigations of secondary effects on PSK bit error rate. In particular, the effect of oscillator stability characteristics on PSK telemetry link performance and the effect of carrier unlock characteristics on PSK telemetry link performance were investigated. Both of these effects are exhibited as phase errors, i.e., incoherence of the reference signal, at the coherent demodulator of the PSK receiving system.

4.2 Results of the Oscillator Stability Investigation

The results of the oscillator stability investigation are contained in Figs. 3, 4 and 5 of Sec. 2. These figures show PLL lock error as a function of loop noise bandwidth for various combinations of oscillator characteristics. An exact determination of phase error due to oscillator instability in each of the two modes of operation (open loop or closed loop transponder mode) is not possible at present because details of the oscillator characteristics are not known. However, it is concluded that $A \approx 0.02$ and $0.032 < B < 0.32$ are appropriate parameters for analysis of closed loop operation provided that the uplink transmitted carrier is referenced to an ultra-stable quartz crystal oscillator. If this is not the case, $A \approx 0.2$ would be more appropriate. For the open loop mode, it is estimated that $0.2 < A < 2$ and, again, $0.032 < B < 0.32$.

With the aid of Figs. 3, 4 and 5, the carrier lock error as a function of loop noise bandwidth can be estimated for the two modes of operation. The carrier lock error, ϕ_ϵ is related to bit error rate in that it acts to reduce the effective energy-to-noise density ratio per bit by a factor $\exp[-\phi_\epsilon^2]$.

4.2.1 Suggested Future Efforts in the Area of Oscillator Stability Analysis

It is recommended that tests be performed in accordance with the technique presented in Appendix A. The purpose of such tests is twofold. First, better estimates of the PIONEER link oscillator parameters can be obtained. These can be used to determine the predominant source of error due to oscillator instability and, further, to determine if the errors due to oscillator instability can be reduced using techniques that are within the present state-of-the-art. Second, the data obtained from such tests can be used to confirm the results of the quasi-theoretical analysis presented in Sec. 2. It is important to note that these results are not in agreement with previous analyses in which it is always assumed that frequency flicker noise is always the predominant form of oscillator instability.

It is also recommended that a theoretical analysis be conducted to determine the optimum method of synthesizing a 2 GHz carrier. Different techniques yield different phase fluctuation characteristics as can be seen by examining the open loop and closed loop transponder performance analyses of Sec. 2. The techniques to be analyzed and compared should include:

1) straightforward frequency multiplication of a reference (1-5 MHz) oscillator output;

2) phase-lock of a microwave source to a reference signal derived by frequency multiplication of a reference (1-5 MHz) oscillator output; and

3) phase-lock of a microwave source, which consists of a VCO (100-400 MHz) and frequency multiplier, to a reference signal derived by frequency multiplication of a reference (1-5 MHz) oscillator output.

Such an investigation would have application to the PIONEER link analysis in addition to its general significance.

4.3 Results of Carrier Unlock Analysis

The effect of carrier unlock on bit error rate is shown in Fig. 6 of Sec. 3. The purpose of this part of the study effort was to determine mechanisms of failure at very low bit rate, i.e., when S/N_o is relatively small. It was found that at low bit rate the signal-to-noise ratio in the carrier tracking loop of the PIONEER link receiver is such that carrier unlock has a significant effect on overall bit error rate. The results shown in Fig. 6 of Sec. 3 are not exact. There are two implicit assumptions. First, it is assumed that while the loop is in a state of unlock, the probability of bit error at the output of the demodulator is 1/2. This would not be correct, for example, if the duration of unlock is substantially shorter than the duration of one bit. It is also assumed, that having unlocked, the PLL moves to the next stable lock point (or possibly the one after that) and relocks in a time which is inversely proportional to the loop noise bandwidth. A range of unlock durations was assumed, namely, $4/B_n$ to $8/B_n$ sec.

4.3.1 Suggested Future Efforts to Improve Low S/N_o Performance

Improvement in oscillator stability performance will allow reduction in carrier loop noise bandwidth. In this way, the signal-to-noise ratio in the loop may be improved. Another method for increasing the signal-to-noise ratio in the loop is to reduce the signal suppression introduced by the limiter at the signal input to the carrier loop phase detector and to reduce the signal suppression in the carrier loop phase detector which is associated with data deviation. These two improvements would increase the effective IF signal-to-noise density ratios by several dB. Examination of Fig. 6 of Sec. 3 shows that an improvement of a few dB in signal-to-noise density would make the effect of carrier unlock almost unnoticeable on bit error rate.

The problem of signal suppression introduced by a limiter at the input to the coherent demodulator has been previously considered.[18]

The approach taken was to estimate the subcarrier square wave and to use this signal to remove the subcarrier at IF. In this way, the bandwidth preceding the coherent demodulator could be reduced significantly in proportion to data bit-rate rather than subcarrier frequency. The technique is described briefly in Appendix B.

It is recommended that the application of this technique to improve carrier loop performance be investigated. Preliminary investigation indicates that the estimate of the subcarrier generated by the decision directed demodulator, described in Appendix B, and possibly the estimate of the data may be used directly to narrow the bandwidth of the IF input to the carrier loop phase detector. Thus, an improvement similar to that gained in the demodulation process may also be applied to the carrier tracking process with a minor hardware effort. The following comparative analyses are suggested. First, it is noted that two techniques are available for removing the modulation at IF given the estimates of the modulation. Namely, the IF signal may be multiplied by the estimates of the modulation, as is done in the decision directed demodulator of Appendix B, or, the estimates of the modulation may be used to PM the reference signal to the carrier tracking loop. This latter technique, in effect, subtracts an estimate of the modulation from the modulation on the IF signal. The two techniques are similar, but not the same. Therefore a comparative analysis of the effectiveness of these techniques should be conducted.

Second, it is noted that the estimate of the data modulation is much less than optimum while the estimate of the subcarrier should be quite good. Thus, it is recommended that the utility of this scheme for carrier loop performance improvement be analyzed for the case of data and subcarrier estimate feedback and for the case in which the subcarrier estimate is used alone. For this latter case, the coupling between data modulation and carrier tracking error must be investigated and methods developed for reducing the coupling at low bit rates.

REFERENCES

1. Baghdady, E.J., Lincoln, R.N. and Nelin, B.D., "Short-Term Frequency Stability: Characterization, Theory and Measurement," Proc. IEEE. Vol. 53, No. 7, July 1965.

2. Cutler, Leonard S., "Present Status in Short Term Frequency Stability," Frequency, Vol. 5, No. 5, p. 13, September/October 1967.

3. Edson, W.A., "Noise in Oscillators," Proc. IRE, Vol. 48, No. 8, pp 1454-1466, August 1960.

4. Golay, Marcel J.E., "Monochomaticity and Noise in a Regenerative Electrical Oscillator," Proc. IRE, Vol. 48. No. 8, pp 1473-1477, August 1960.

5. Special Issue on Frequency Stability, Proc. IEEE, Vol. 54, No. 2, February 1966.

6. "Short-Term Frequency Stability," Proceedings of the IEEE-NASA Symposium, GSFC; NASA Publication SP-80, November 1964.

7. Leeson, D.B., "A Simple Model of Feedback Oscillator Noise Spectrum," Ref. 8 (correspondence) pp 329-330.

8. Attkinson, W.R., Fey, L., and Newman, J., "Spectrum Analysis of Extremely Low Frequency Variations of Quartz Oscillators," Proc. IEEE (correspondence) Vol. 51, No. 2, p. 379, February 1963.

9. Allan, David W., "Statistics of Atomic Frequency Standards," Ref. 8, pp 221-230.

10. Baghdady, E.J., Lectures on Communication Theory.

11. Van Blerkom, R., and Anema, S.L., Considerations for the Short Term Stability of Frequency Multipliers.

12. Malling, L.R., Phase-Stable Oscillators for Space Communication, Including the Relationship Between the Phase Noise, the Spectrum, the Short Term Stability, and the Q of the Oscillator, Proc. IRE, July 1962.

13. Sydnor, R. et al, Frequency Stability Requirements for Space Communication and Tracking Systems, Proc. IEEE, February 1966.

REFERENCES (Continued)

14. ADCOM, Inc., Design of the White Sands Range and Range Rate System: Final Report, Contract No. DA-31-125-ARO-D-393, Mod 6, October 21, 1967 for WSMR, New Mexico.

15. Applied Technology, Model LO-100 series.

16. Cutler, L.S. and Searle, C.L., Some Aspects of the Theory and Measurement of Frequency Fluctuation in Frequency Standards, Proc. IEEE, February 1966.

17. Gardner, F.M., Phaselock Techniques, p 25, Wiley, 1966.

18. JPL SDA Engineering Pre-release, August 16, 1968.

Appendix A

MEASUREMENT SYSTEM FOR $S_{\phi}(\omega)$

Principle of Operation

The basic configuration of the measurement system consists of three functional sections as shown in Fig. A.1: the signal extraction and processing section, the error multiplication section, and the output analysis section.*

It has been shown* that the requisite rejection of the average-frequency (f) cannot be achieved with one oscillator signal alone. Thus, two independent oscillators, generating two 1 MHz oscillations at almost identical average frequencies, supply inputs to the measurement system. An automatic detection loop, incorporated in the signal extraction and processing section, maintains a synchronous quadrature relationship between these two signals, thus essentially removing all average frequency drifts.

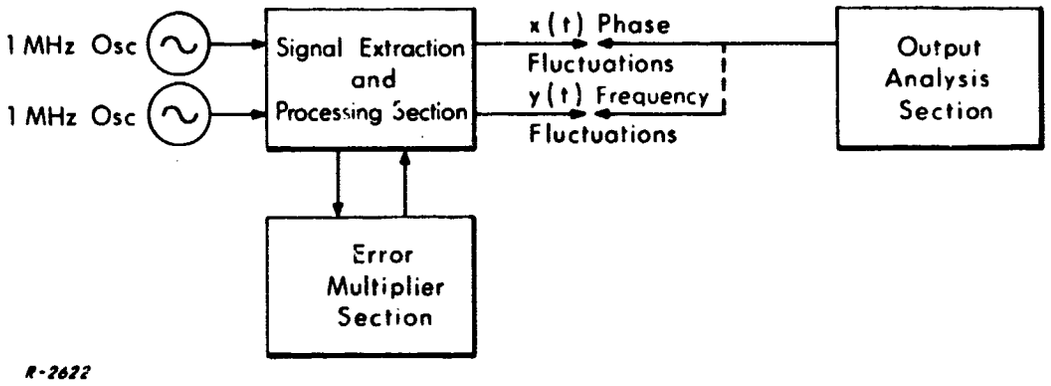

Fig. A.1 Basic Configuration of the Measurement System

*ADCOM, Inc., "Theory, Characterization, and Measurement of Short-Term Frequency Stability with Application to Frequency Synthesis," Final Report, Task No. ASTR-AD-2, Contract No. NAS8-11228, NASA report for George C. Marshall Space Flight Center, Huntsville, Alabama, 31 December 1964.

The automatic-detection loop, illustrated in simplified form by Fig. A.2 is essentially a second-order electromechanical phase-locked loop. The motor and RF resolver operate on one of the two input oscillations to simulate a VCO. The average frequency difference between the two oscillators, denoted by $\Delta\bar{f}$ and representing the relative phase drift between the two oscillators, can be seen to be analogous to a doppler offset frequency in a conventional tracking PLL.

The particular implementation of the automatic-detection loop shown in Fig. A. 2 has certain desirable properties. The loop has been designed so that the locked-loop transference from input frequency difference to the lowpass output y(t) is maximally flat (second-order Butterworth). Thus, this output is analogous to an FM discriminator output for all difference-frequency fluctuation components occupying the spectrum from dc almost up to ω_c, the loop cutoff frequency. However, it has certain advantages over an FM discriminator output. First, there is no long term or temperature-dependent center-frequency drift. Second, because of the loop lowpass characteristic, the high-frequency fluctuation components are greatly attenuated (at 12 dB per octave). Third, the basic sensitivity before dc gain of 2π volts per hertz is very high.

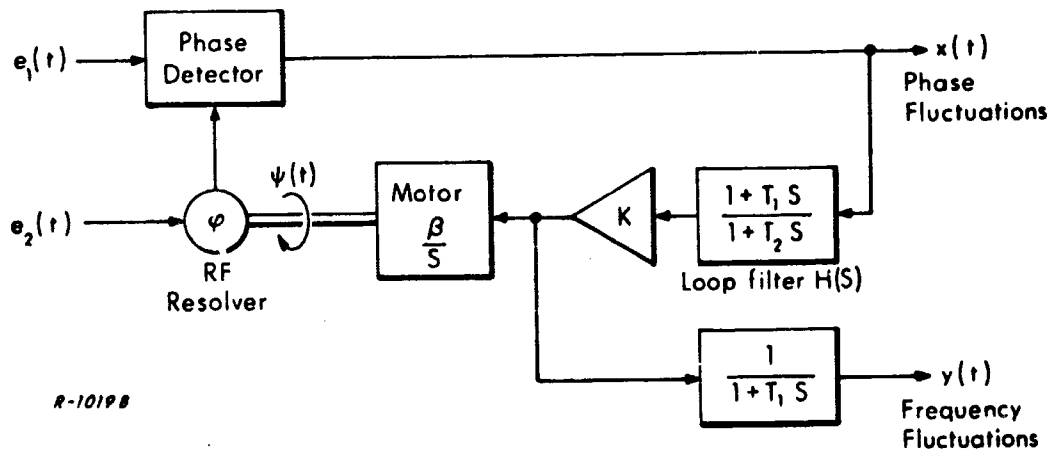

Fig. A. 2 Basic Configuration of the Automatic-Detection Loop

The locked-loop transference from input phase difference to the high-pass output x(t) is flat from frequencies slightly greater than ω_c. Thus, this output is analogous to a phase detector output, but it too has certain advantages over conventional open-loop techniques. Since the signals are continuously maintained in quadrature at the detector, several problems are eliminated. First, there is no variation in the phase-to-voltage transference with changing phase. Second, the rejection of AM components is maximized, and this too, does not vary with changing phase. Third, there is no abrupt change in the output signal at 2π intervals as happens in open-loop systems. In addition to these advantages, the system possesses a high phase-to-voltage sensitivity of 10 volts per radian before post-amplification which, combined with a low noise level, provides very high signal-to-noise ratio.

The automatic-detection loop thus provides two output signals: the first, x(t), is a signal proportional to the phase-difference fluctuations passed through a maximally-flat highpass filter; while the second, y(t), is a signal proportional to the frequency-difference fluctuations passed through a maximally-flat lowpass filter. These two output signals are fed, after amplification and interfacing, to the output analysis section.

The output analysis section contains primarily a low-frequency spectral-density analyzer, which can process either x(t) or y(t) and graphically display the corresponding spectrum. Spectral analysis at frequencies below the lower frequency limit of the analyzer can be accomplished by recording and digital processing of the fluctuations. Providing that the statistical independence of all oscillator fluctuations is assured, two-at-a-time measurements upon three oscillators are sufficient to determine the fluctuation spectra of each.

The predetection error multiplier section is a group of frequency multipliers and mixers operating on the two 1 MHz oscillator signals whose phase or frequency fluctuation spectra are to be measured. Error multiplication

provides effective predetection gain on the phase and frequency fluctuations, and hence an increase of the overall sensitivity of the measurement system, where sensitivity is defined as the lowest spectral densities $S_\phi(\omega)$ or $S_{\dot{\phi}}(\omega)$ that can be reliably measured. To couple properly with the automatic detection loop, the error multiplier accepts 1 MHz signals as inputs and provides 1 MHz signals as outputs with enhanced phase and frequency fluctuations.

Appendix B

OPERATION OF A DECISION DIRECTED DEMODULATOR

For the purposes of discussion, a simplified block diagram of the device is shown in Fig. B.1. The device operates as follows.

The IF input to the subsystem is

$$e_{if}(t) = \cos[\omega_{if}t + \delta a(t)b(t)] \tag{B-1}$$

where δ is the modulation deviation, $a(t) = \pm 1$ is the data modulation and $b(t) = \pm 1$ is a subcarrier square wave. Expanding,

$$e_{if}(t) = \sin[\delta a(t)b(t)]\cos\omega_{if}t - \cos[\delta a(t)b(t)]\sin\omega_{if}t$$

$$= a(t)b(t)\sin\delta\cos\omega_{if}t - \cos\delta\sin\omega_{if}t \tag{B-2}$$

Assume for the moment that the estimate at the subcarrier $\hat{b}_i(t) \approx b(t)$. Then, the output of the upper narrow IF amplifier will be

$$e_1(t) \approx a(t)\sin\delta\cos\omega_{if}t \tag{B-3}$$

Note that the narrow IF amplifier need only be wide enough to pass a(t). The IF reference signal to which the carrier loop is locked is used to demodulate $e_1(t)$ yielding the video data output a(t).

The IF signal, $e_{if}(t)$, is multiplied by $\hat{a}(t)\,\hat{b}_q(t)$ in the lower channel. $\hat{a}(t)$ is a relatively crude estimate of the data modulation a(t) and $\hat{b}_q(t)$ is the quadrature version of the subcarrier estimate. Assuming that $\hat{a}(t) \approx a(t)$, the output of the lower narrow IF amplifier is of the form

$$e_2(t) = [b(t)\hat{b}_q(t)]_{LP}\sin\delta\cos\omega_{if}t \tag{B-4}$$

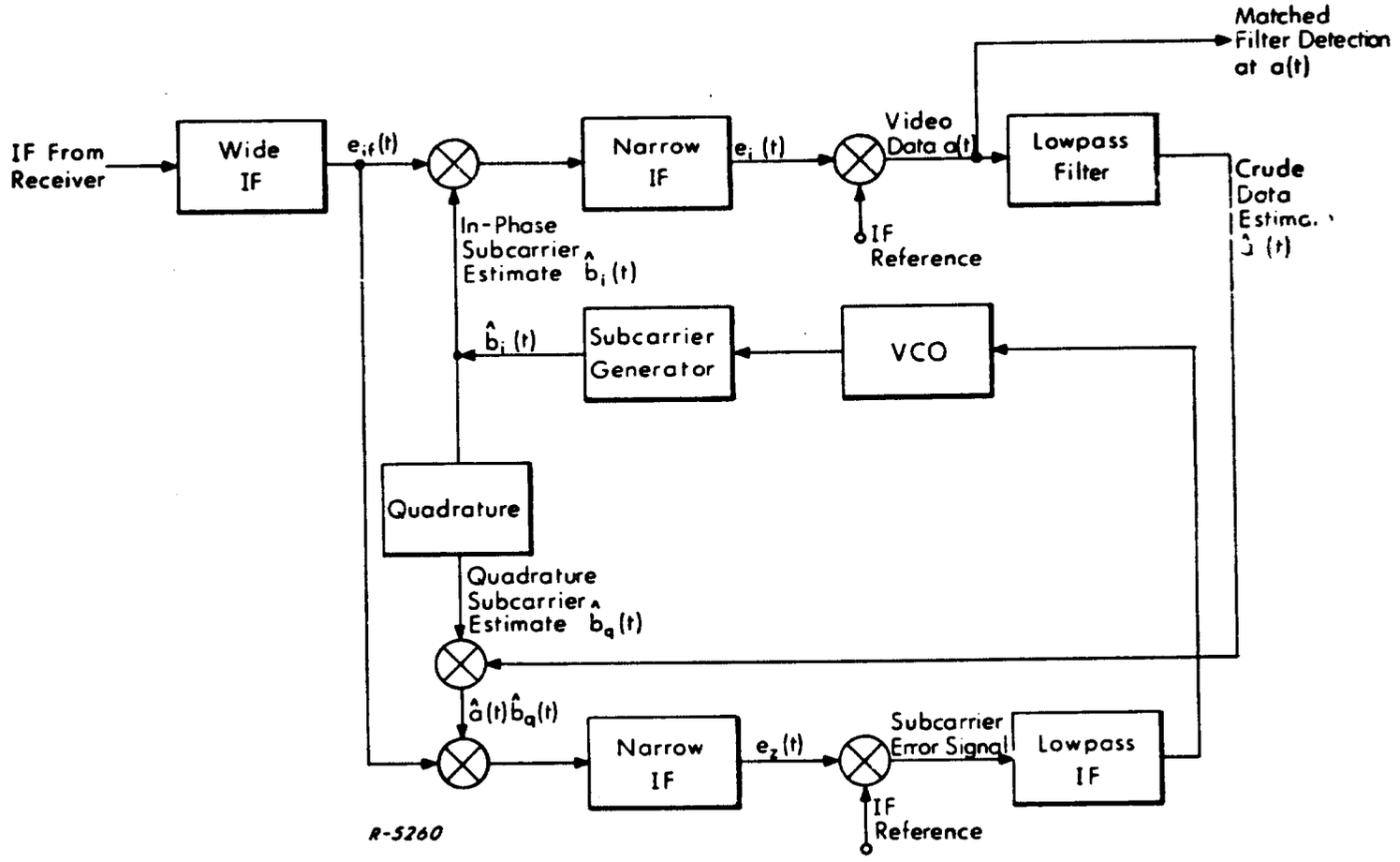

Fig. B. 1 Simplified Block Diagram of the SDA

where the symbol $[\ ]_{LP}$ is used to indicate lowpass filtering. Thus, if $\hat{b}_i(t)$ is exactly in-phase or out-of-phase with b(t) the subcarrier error signal will be zero. While, if $\hat{b}_i(t)$ is actually in quadrature with b(t) the subcarrier error signal will be proportional to either, + sin δ or - sin δ depending on whether b(t) leads $\hat{b}_i(t)$ or vice versa. The subcarrier error is therefore recognized as a suitable error signal for a phase-locked loop which tracks the subcarrier waveform. In this way $\hat{b}_i(t)$ is generated.

The technique used to acquire the decision directed demodulation employs a third IF channel not shown in Fig. B.1. The technique is based on the fact that the magnitude of the output of each of the IF amplifiers is a function of the coherence of b(t) and $\hat{b}_i(t)$, as noted above. It need only be said that once the unit acquires, it is possible to filter the data signal at IF in a narrower bandwidth preceding coherent detection thus improving threshold performance.